

# XENON POROMETRY

A NOVEL METHOD FOR CHARACTERIZATION OF POROUS MATERIALS BY  
MEANS OF  $^{129}\text{Xe}$  NMR SPECTROSCOPY OF XENON GAS DISSOLVED IN A  
MEDIUM

VILLE-VEIKKO TELKKI

*Department of Physical Sciences  
University of Oulu  
Finland*

Academic Dissertation to be presented with the assent of the Faculty of Science,  
University of Oulu, for public discussion in Auditorium L10 (Raahensali), on February  
10<sup>th</sup>, 2006, at 12 o'clock noon.

OULU 2006 • UNIVERSITY OF OULU

Communicated by

Professor Alexander Pines  
Professor Roderick Wasylishen

ISBN 951-42-7991-3 (PDF)  
ISBN 951-42-7965-4

ISSN 1239-4327

OULU UNIVERSITY PRESS  
OULU 2006

**Telkki, Ville-Veikko: Xenon porometry, a novel method for characterization of porous materials by means of  $^{129}\text{Xe}$  NMR spectroscopy of xenon dissolved in a medium**

Department of Physical Sciences, University of Oulu, P.O.Box 3000, FI-90014  
University of Oulu, Finland

*Report Series in Physical Sciences No. 37 (2006)*

***Abstract***

The present thesis describes the development of a novel method, referred to as xenon porometry, for the determination of the structural properties of porous materials by means of xenon NMR spectroscopy. The method exploits the high sensitivity of the chemical shift of the  $^{129}\text{Xe}$  isotope to its local environment. The purpose of the medium added to the sample is to slow down the diffusion of xenon so that the NMR signal of a xenon atom is characteristic of the properties of one pore, and the signals of all the atoms in the sample represent the distribution of the properties.

Two types of porous materials (controlled pore glasses and silica gels) with well-known properties and three different media (acetonitrile, cyclohexane, and naphthalene) were used in the studies. The behavior of the medium and dissolved xenon at different temperatures around the melting point of the medium was explained. By varying the pore size of the material, three different correlations that make it possible to measure the pore sizes of unknown materials were experimentally determined. The chemical shift of xenon inside pockets built up in the pores during solidification of the medium turned out to be especially sensitive to pore size, and this correlation makes it possible to determine the pore size distribution. The curious behavior of the chemical shift as a function of pore size was explained by using a model based on the fast exchange between xenon adsorbed on the walls of the pockets and free xenon in the middle of the pockets. It was also proved that the porosity of the materials can be determined by comparing the intensities of two signals originating from xenon dissolved in a liquid medium.

A comparison of the xenon porometry method with other methods used for pore size characterization leads to the following conclusions: The range of applications of the method is relatively wide, the measurements are fast and easy to do, the analysis of the spectra is simple on the basis of the information presented in this thesis, and the properties of the materials can be extracted from the spectral data with basic mathematical conversions. Because there are several different types of correlations available in the same spectra that represent the properties of the porous material, the complementary information of all the correlations make it possible to obtain a picture of the structures of very complex systems.

Keywords: nuclear magnetic resonance spectroscopy, porous materials, xenon porometry,  $^{129}\text{Xe}$ .



## Acknowledgements

The present study was carried out in the Department of Physical Sciences at the University of Oulu. I am grateful to the department and its head professor Jukka Jokisaari for placing the facilities at my disposal. Professor Jokisaari was also my professionally skilled and creative supervisor, and he introduced the idea for the investigation of the novel method presented in this thesis. I am very grateful to him for the fruitful and pleasant cooperation. Besides Professor Jokisaari, Docent Juhani Lounila is another person who has contributed to all the papers presented in this thesis. His extremely wide knowledge of fundamental physics as well as his unfailing logical thinking ability has been of great benefit in discovering the explanations of the new phenomena observed in the measurements and in constructing theories. I am deeply indebted to him for the long discussions and excellent cooperation.

I want to thank Dr. Tuomas Koskela for his guidance in the worlds of experimental NMR spectroscopy and xenon NMR. I have had an opportunity to work in the NMR laboratory of the University of Oulu. I am grateful to the former laboratory managers Petri Ingman and Harri Koskela and the present manager Anu Kantola for their help in the technical and scientific problems encountered in the laboratory. I was lucky to be able to do my postgraduate studies in the NMR research group, where the atmosphere is warm and supportive and the people are friendly and fair-minded. In addition to the persons mentioned above, I would like to thank the following colleagues: Henri, Jani, Jussi, Joonas, Jyrki, Matti, both Pekkas, Perttu, Päivi, Sami, Susanna, and Teemu.

I gratefully acknowledge the financial support of this work by the Vilho, Yrjö, and Kalle Väisälä Foundation, the Tauno Tönning Foundation, the Faculty of Science of the University of Oulu, and the Magnus Ehrnrooth foundation. I am thankful to Keith Kosola for excellent language review.

Finally, I would like to express my deepest gratitude to my wife Heidi for her love and support. Special thanks also belong to my parents and siblings for caring. And great thanks to my friends for the relaxing time spent outside of work.

Berkeley, California, November 2006

Ville-Veikko Telkki

## List of original papers

The present thesis consists of an introductory part and the following papers, which are referred to in the text by their Roman numerals.

- I Telkki V-V, Lounila J & Jokisaari J (2005) Behavior of Acetonitrile Confined to Mesoporous Silica Gels As Studied by  $^{129}\text{Xe}$  NMR: A Novel Method for Determining the Pore Sizes. *Journal of Physical Chemistry B* 109: 757-763.
- II Telkki V-V, Lounila J & Jokisaari J (2005) Determination of Pore Sizes and Volumes of Porous Materials by  $^{129}\text{Xe}$  NMR of Xenon Gas Dissolved in a Medium. *Journal of Physical Chemistry B* 109: 24343-24351.
- III Telkki V-V, Lounila J & Jokisaari J (2006) Xenon Porometry at Room Temperature. *Journal of Chemical Physics*, in press.
- IV Telkki V-V, Lounila J & Jokisaari J (2006) Influence of Diffusion on Pore Size Distributions Determined by Xenon Porometry. Submitted to *Physical Chemistry Chemical Physics*.

In these papers, the present author has performed all the experimental work, including sample preparation, measurements on NMR spectrometers, and analyses of the spectra. In addition, the initial versions of the manuscripts were written by the author. All the manuscripts were finished as teamwork.

## Contents

Abstract	
Acknowledgement	
List of original papers	
1 Introduction .....	8
1.1 Outline of the thesis.....	9
2 NMR spectroscopy .....	11
2.1 Basics of NMR spectroscopy.....	11
2.2 Xenon NMR .....	12
2.3 Chemical exchange.....	13
3 Porous materials .....	15
3.1 Controlled pore glass.....	15
3.2 Silica gel .....	16
3.3 Methods for characterization of porous materials .....	17
3.3.1 Mercury porosimetry .....	17
3.3.2 Gas Adsorption .....	18
3.3.3 NMR relaxometry.....	19
3.3.4 NMR cryoporometry .....	20
4 Xenon porometry.....	21
4.1 Sample .....	21
4.2 Spectra .....	22
4.3 Pore size determination using a solid medium .....	23
4.4 Pore size determination using a liquid medium.....	25
4.5 Pore size determination by melting point depression .....	27
4.6 Porosity determination.....	28
5 Conclusions .....	30
References .....	32
Original papers .....	34

## 1 Introduction

Porous materials are solids that contain networks of pores and cavities. Usually the internal surface area consisting of the walls of the pores is much larger than the external surface area, and this gives the materials extraordinary adsorption properties. Porous materials have an important role in many natural processes. In addition, they are widely used in industrial applications such as catalysis, chromatography, fluid transport and storage, or as composite materials for structural purposes. The materials are classified according to their pore size as microporous (pore diameter smaller than 20 Å), mesoporous (diameter between 20 and 500 Å), and macroporous (diameter larger than 500 Å), and each class has its own characteristic adsorption properties. To be able to use the materials appropriately, it is essential to have reliable and efficient methods for characterizing them. Pore size distribution, total pore volume, specific surface area, gas and liquid permeability, and pore tortuosity are examples of important properties of porous materials. [1]

The properties of porous materials were studied in the present thesis project by means of nuclear magnetic resonance (NMR) spectroscopy [2-4]. In a conventional NMR experiment, a sample is exposed to a strong, static magnetic field generated by current in a superconducting coil, and the thermal equilibrium of nuclear spins of atoms is disturbed by radio frequency radiation. The frequencies emitted by the spin system after the disturbance reveal what kinds of NMR active nuclei the sample contains, but, what is much more interesting, they also contain information about the *surroundings* of the nuclei. This makes NMR spectroscopy pervasive in the sciences. For instance, NMR is the only method for determining the molecular structure of a substance in a solution. The most famous application of NMR is the magnetic resonance imaging (MRI) technique, in which a static magnetic field is intentionally made inhomogeneous in order to add spatial information to the NMR signal. The method makes it possible, for example, to reconstruct the cross-sectional images of the human brain without causing any damage to the patient. NMR spectroscopy is eminently suitable for materials research because it provides information from the molecular level to the macroscopic scale, and the information can also be obtained from inside opaque materials. In addition, it does not destroy the material.



This thesis focuses on the development of a novel method, called xenon porometry, for the characterization of porous materials. The NMR resonance frequency of the  $^{129}\text{Xe}$  isotope of a xenon atom is extremely sensitive to its local environment, and this sensitivity has been widely utilized in studies of porous materials. However, due to the fast diffusion of the absorbed gas, the observed signal is an average of the properties of the large amount of pores sampled by the atoms during the time scale of the NMR measurement. In our studies, we slowed down the diffusion of xenon by immersing the porous material in a liquid or solid medium. Then the resonance frequency of a xenon atom represents the properties of a single pore more accurately, and the signals observed from the different pores together represent the distribution of the properties.

The measurements were made using well-known commercial silica-based porous materials (controlled pore glasses and silica gels) with the possibility to vary certain properties in order to identify their effects on the NMR signals. This also enables the determination of correlations between the properties and the parameters of the NMR signals, and the correlations can be used further in the characterization of unknown materials. The studies conducted in this thesis project prove that xenon porometry is especially applicable in the determination of the pore size distribution of materials, and this determination is very simple, quick and straightforward compared with other traditional methods.

## 1.1 Outline of the thesis

This thesis is a wide introduction to the xenon porometry method. The most significant part of the work is contained in papers I – IV. Some aspects necessary for understanding the details in the papers are presented in the following chapters. Chapter 2 deals with NMR spectroscopy, and it focuses on the essentials of xenon NMR, such as chemical shift and chemical exchange phenomena. Reliable interpretation of the results of NMR measurements requires accurate knowledge about the properties of the porous materials in the sample. Hence, the processes used to prepare the materials are described in chapter 3. In order to have objects of comparison in the discussion of the usefulness of xenon porometry, some traditional methods for the characterization of porous materials are introduced in the same chapter. This discussion is included in the conclusion part in chapter 5. The basics of the xenon porometry method are summarized in chapter 4.

Paper I describes the first xenon porometry experiments. Acetonitrile was used as the medium and silica gels as the porous materials, and the spectra were measured over a wide temperature range. The main impact of this work is that it explains the complicated behavior of the medium and dissolved xenon around the phase transition points of the medium, thus making it possible to specify the origins of the signals in the spectra. It was also shown that the chemical shift of the signal of xenon dissolved in a confined liquid (referred to as signal C, see the spectra in section 4.2 Figure 3) and that of a signal appearing below the freezing point of a confined medium (signal D) are sensitive to pore size, thus providing two new possibilities for determining the pore size of unknown materials. Furthermore, it was proved that the appearance or disappearance and the intensity changes of certain signals reveal the melting point of the medium in the pores

and outside the porous material, which opens up the third possibility for estimating pore sizes. The effects of the liquefaction of xenon at the lowest measurement temperatures were also explained and modeled.

In paper II, correlations between pore size and the chemical shifts of signals C and D were investigated using an extensive set of measurements with a variety of porous materials. Besides silica gels, controlled pore glasses with sharp and well-defined pore size distributions were used as model materials. By comparing the spectral information with the properties of the materials announced by manufacturers, it was shown that the chemical shift of signal D is especially sensitive to pore size, and its shape represents well the pore size distribution function. In addition, it was proved that the porosity of the material can be determined from the intensity of signal C. When acetonitrile is replaced by cyclohexane in the sample, the sensitivity to pore size of the chemical shift of signal C increases, but the most sensitive signal for pore size determination (signal D) does not appear. The paper also contains a study of the influence of xenon gas on the melting points of the medium and an investigation of hysteresis observed in the cooling-warming cycle.

Paper III introduces a new medium, naphthalene, which makes it possible to determine pore sizes by means of signal D near room temperature. The curious behavior of the chemical shift of signal D as a function of pore radius was successfully explained by using a model based on the fast exchange between xenon atoms on the walls of pockets built up inside the pores and non-adsorbed atoms in the middle of the pockets. The chemical shifts were compared with those measured from samples containing only porous materials and xenon gas without any medium. In addition, the dependence of the chemical shift of signal D on the pressure of xenon in the sample was also studied.

Paper IV concentrates on an investigation of the exchange processes in the xenon porometry sample using two-dimensional exchange spectroscopy. The results support the basis assumption in the pore size distribution determination that a solid medium prevents the xenon atoms from moving between different pores. In addition, the results imply that, when acetonitrile is used as a medium, the diffusion of xenon dissolved in a liquid medium is so slow that the chemical shift of a xenon atom is characteristic of one pore size, and the shape of the composite signal of all the atoms in the sample represents quite well the pore size distribution, as in the case of signal D.

## 2 NMR spectroscopy

### 2.1 Basics of NMR spectroscopy

Spectroscopy is the study of the interaction between electromagnetic radiation and matter. In NMR spectroscopy [2-4], the matter is usually immersed in a large static magnetic field  $\mathbf{B}_0$ , and the interactions of the spin angular momentum  $\mathbf{I}$  of the nuclei with the local magnetic field and electric field gradient are studied by disturbing the equilibrium in the sample by using radio frequency pulses.

The nuclear Hamiltonian describing the interaction with the local magnetic field  $\mathbf{B}_{\text{loc}}$  at the nuclear site is proportional to the dot product between the spin angular momentum operator and  $\mathbf{B}_{\text{loc}}$ :

$$H = -\gamma\hbar\hat{\mathbf{I}} \cdot \mathbf{B}_{\text{loc}}. \quad (1)$$

Here,  $\gamma$  is the gyromagnetic ratio and  $\hbar = h/2\pi$ , where  $h$  is Planck's constant.

The local field  $\mathbf{B}_{\text{loc}}$  experienced by the nucleus is not the same as the static magnetic field  $\mathbf{B}_0$ , because surrounding nuclei and electrons cause small changes in the field. For instance, the external magnetic field may induce currents in the electron cloud of the atom or molecule, and the currents in turn generate a small magnetic field that changes the local field experienced by a nucleus. The different local fields of the nuclei are reflected in the observed NMR spectrum as different resonance frequencies, and this makes NMR spectroscopy a very powerful method in the investigation of local surroundings.

The change in the resonance frequency due to the field created by the electrons is called a chemical shift. It consists of diamagnetic and paramagnetic parts. The diamagnetic contribution is due to currents in the electronic ground states, and it arises dominantly from the core electrons. The diamagnetic field attenuates the total magnetic field. The paramagnetic term is a consequence of electron movements in excited electronic states, and it is highly dependent on the nuclear environment. It increases the total magnetic field.

## 2.2 Xenon NMR

Xenon has two NMR active isotopes,  $^{129}\text{Xe}$  and  $^{131}\text{Xe}$ , and their natural abundances are relatively large (26.4 and 21.2 %, respectively). The spin of the former isotope is 1/2, which makes it experimentally favorable. However, the quadrupolar  $^{131}\text{Xe}$  isotope (spin 3/2) is suitable, for example, for the study of electric field gradients. In this work, only the  $^{129}\text{Xe}$  NMR spectra were measured, and hereafter all the discussions concerning xenon NMR refer to NMR of the  $^{129}\text{Xe}$  isotope.

Xenon is an inert noble gas. It has a large, polarizable electron cloud, which makes its chemical shift very sensitive to the local environment. Therefore, xenon is an ideal probe atom. It has been used in studies of the properties of gases, liquids, liquid crystals, polymers, clathrates, porous materials, and surfaces [5-7]. The sensitivity of xenon can be increased by several orders of magnitude by an optical pumping procedure [8,9], and this hyperpolarization has considerably extended the range of applications of xenon NMR, enabling, for example, magnetic resonance imaging of xenon gas absorbed in materials.

As far as porous materials are concerned, xenon NMR has been utilized in the investigation of pore sizes, geometries, and adsorption properties of materials, and in probing the effects and locations of other adsorbates and cations in the materials, among other applications. Fraissard and coworkers [10,11] have proposed that the chemical shift of xenon absorbed in a porous material consists of the sum of shifts caused by various interactions:

$$\delta_{obs} = \delta_0 + \delta_S + \delta_{Xe} + \delta_{SAS} + \delta_E + \delta_M. \quad (2)$$

Here,  $\delta_0$  is the shift of gaseous xenon and  $\delta_S$  is the shift caused by the framework, both at zero pressure.  $\delta_{Xe}$  represents the Xe-Xe interactions and it depends on pressure.  $\delta_{SAS}$  is a consequence of strong adsorption sites in the material, and  $\delta_E$  and  $\delta_M$  are shifts caused by the electric and magnetic fields of paramagnetic cations, respectively. Because the diffusion of xenon gas inside a porous material is usually very fast, the chemical shift reflects an average of the shifts in all the environments where xenon has been during the time scale of NMR measurement.

Besides the other things mentioned above, the chemical shift of absorbed xenon has been found to be dependent on average pore size. Several correlations between the chemical shift and the pore size of microporous materials have been suggested [12-14]. Terskikh and coworkers measured the chemical shift of xenon absorbed in a large amount of silica-based mesoporous materials, and they explained the behavior of the chemical shift as a function of pore size by means of a model based on a fast exchange of xenon atoms between the adsorbed site on the pore wall and the free site in the middle of the pore [15,16]. The model was also utilized in the analysis of the results obtained from NMR porometry experiments in this thesis project, and its details were presented in Paper IV.

## 2.3 Chemical exchange

The transfer of atoms or molecules between different environments is called a chemical exchange. In NMR spectroscopy, the different environments may be observed in chemical shifts, couplings or relaxation times. In the simplest case, the chemical exchange takes place between two sites in which the difference between the resonance frequencies of uncoupled spin  $\frac{1}{2}$  nuclei is  $\Delta\nu$ . If the mean lifetime  $\tau_1$  of the nucleus in one site is much longer than the reciprocal of  $\Delta\nu$ , the exchange is slow, and separate sharp resonance signals are observed from both sites. On the other hand, if  $\tau_1$  is much shorter than the reciprocal, a fast exchange between the sites takes place, and only one signal is observed. The resonance frequency of the signal is an average of the resonance frequencies of the sites weighted by their populations. If  $\tau_1$  increases continuously from a slow to a fast exchange region, the separated signals first broaden, then they gradually merge together, and finally a sharp exchange signal is observed. [17]

Two-dimensional exchange spectroscopy (2D EXSY) is a useful method for investigating exchange processes if the exchange is fast compared to the longitudinal relaxation time and slow compared to the spectral parameters affected by the exchange [3,18]. The pulse sequence of the method is shown in Figure 1. In the 2D EXSY experiment, the magnetization of different sites is frequency labeled during the evolution period and stored as a longitudinal magnetization. If the exchange between the different sites takes place during the mixing period, the observed frequency in the detection period differs from that in the evolution period. Hence, the appearance of off-diagonal signals (called also cross-peaks) in the Fourier transformed 2D spectrum is a mark of an exchange between the sites. A series of 2D EXSY experiments with different mixing times may reveal the exchange pathways and time scales in the sample. However, in interpreting the spectra one has to take into account that an exchange taking place through different intermediate sites during a certain mixing time causes a similar signal as a direct exchange between the initial and final sites. In addition, cross-relaxation, quadrupolar relaxation, and chemical reactions may also cause changes in the intensities of cross-peaks.

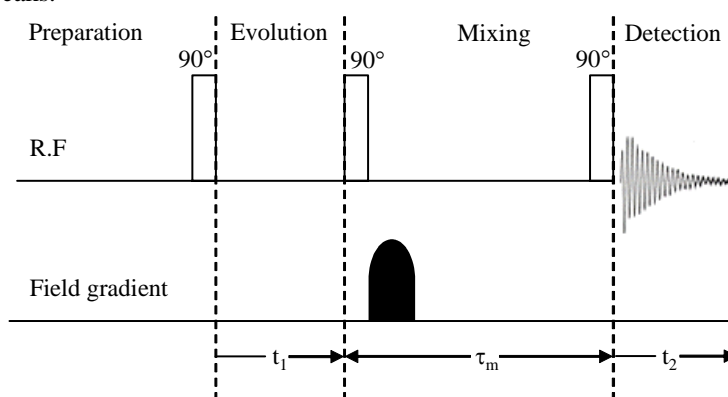


Figure 1. 2D EXSY pulse sequence.

The disadvantageous residual transverse magnetization after the evolution period is destroyed by a gradient pulse in Figure 1, but alternatively it can be destroyed by phase cycling. The spurious effects caused by an imperfect  $90^\circ$  pulse can also be minimized or eliminated by phase cycling.

### 3 Porous materials

When analyzing the phenomena observed from the xenon porometry sample and determining the correlations between the spectral data and certain properties, it is necessary to know as accurately as possible the properties of the materials used in the model so that the information can be used later for reliable characterization of unknown materials. Therefore, this chapter concentrates on a description of the preparation processes and the properties of controlled pore glass and silica gel materials used in this study. Scanning electron microscope images of the materials are shown in the references given in the text. Traditional methods (mercury porosimetry and gas adsorption) and two NMR methods (NMR relaxometry and cryoporometry) used to characterize porous materials are also presented so that their advantages and weaknesses can be compared with those of xenon porometry.

#### 3.1 Controlled pore glass

Glass can be defined, for example, by its molecular structure or by a kinetic description, but in this context the following definition is suitable: "Glass is a substance in a condition which is continuous with, and analogous to, the liquid state of that substance, but which, as the result of a reversible change in viscosity during cooling, has attained so a high degree of viscosity as to be for all practical purposes rigid." [19] Glass is a liquid that has been cooled below its crystallization point without crystallization having occurred. Because it is a solidified liquid, it is very homogeneous.

Controlled pore glass [20,21] is a fine powder consisting of rigid porous particles of almost pure silica. The pores are interconnected and the network of the pores permeates through the particles. The mean pore diameter of the material can vary from 75 to 3000 Å. The pore size distribution of the material is very sharp; usually at least 80 % of the pores have a diameter within  $D_0(1 \pm 0.1)$ , where  $D_0$  is the mean pore diameter. The typical pore volume of the material is 1 cm<sup>3</sup>/g. Its specific surface area is inversely proportional to the mean pore diameter, and it varies from 10 to 200 m<sup>2</sup>/g with decreasing mean pore size.

The preparation of CPG materials is based on the fact that some liquids are completely miscible above a certain critical temperature  $T_C$ , but below this temperature they separate into different phases. For example, two liquids A and B are miscible in every ratio above  $T_C$ , forming one homogeneous liquid  $M_1$ . When the temperature is lowered enough below  $T_C$ , liquid  $M_1$  begins to segregate into two liquids  $M_2$  and  $M_3$ . Both of the new liquids are still mixtures of liquids A and B, but the concentration of liquid A is high in one mixture and that of liquid B in the other mixture. The concentration ratios are determined by a so-called immiscibility curve. In a system of three liquids, the immiscibility curve becomes an immiscibility surface.

In principle, the terminal stage of the liquid separation is two layers of immiscible liquids. However, the viscosity of the liquid can be increased significantly by supercooling it, after which phase separation takes place very slowly due to slow diffusion. At a certain stage the phase separation process can be completely interrupted by cooling the liquid below the glass transition temperature, because then all motion and diffusion freezes. In this intermediate stage, two phases are interlocked instead of forming different layers. One phase may form spherical droplets that are regularly distributed in the other phase, or both phases may be interconnected, forming a continuous network that is interlocked with the other phase. The dimensions of the phase separation regions may be very small, even on the order of Ångströms.

In CPG preparation, a three-component  $B_2O_3$ - $SiO_2$ - $Na_2O$  system is used. First, a homogeneous mixture of the three liquids is made by increasing the temperature of the system above  $T_C$ . Subsequently, the mixture is cooled down rapidly below the glass transition temperature in order to minimize phase separation in this stage. Then the system is reheated from hours to several days to obtain the phase separation. During the heating, the system segregates into silica-rich and alkali borate-rich phases, and both of them are interconnected phases. The reheating temperature history defines the dimensions of the phases. Next, a homogeneous powder is made by crushing the glass and sieving the particles of a desired size. Finally, the alkali borate-rich phase is decomposed by one acid, and the colloidal precipitate of silica remaining from this phase is removed by another acid in order to achieve the porous network.

Consequently, the dimensions of the pores of the obtained CPG material are mainly defined by the heating temperature function during the phase separation. The above process makes it possible to precisely control the mean pore size, and the pore size distribution of the resulting material is very sharp.

### 3.2 Silica gel

Like CPG, silica gel is a granular porous form of silica. However, the porous structures of these materials differ significantly due to the different ways of preparation, and the properties of silica gels are not as well controlled as those of CPGs. For instance, the pore size distribution of silica gels is much wider than that of CPGs. Silica gels are still very usable in various applications, and the fact that they are very cheap increases their attraction. Small silica gel bags can even be found in new shoes, where they act as a desiccant that absorbs moisture.



Silica gels are synthesized by a sol-gel process, in which a system of colloidal liquid (sol) is transformed into gel, and then the solvent is removed in order to obtain a rigid porous structure [22,23]. The precursors (starting compounds) for the preparation of a colloid consist of a silicon atom surrounded by ligands. Usually, silicon tetraethoxide (TEOS),  $\text{Si}(\text{OC}_2\text{H}_5)_4$ , has been used as the precursor. Due to hydrolysis and condensation reactions, polymeric clusters or small dense silica particles begin to grow in the solution. Generally, polymeric silica sols are obtained from hydrolysis in nonaqueous solutions, whereas particulate silica sols are formed in aqueous solutions. The gel is formed when the size of the polymer increases so much that it extends throughout the solution. Particulate sols can also form a gel, when attractive dispersion forces (van der Waals forces) cause particles to stick together so that they form a network throughout the sample.

The process of changes in the structure and properties after gelation is called aging. Polymerization continues during aging, and its rate depends on the temperature, concentration, and pH of the solution. Polymerization stiffens and strengthens the network by forming new bridging bonds. The solubility of the silica particles depends on the curvature of the surface; the larger the curvature, the larger the solubility. Changes caused by differences in solubility during aging are called coarsening. The small particles dissolve because their curvature is large, and the solute precipitates onto the larger particles. The curvature in the crevices and necks between the particles is negative, leading to low solubility. Thus, material accumulates in those places, strengthening the gel structure and filling the small pores. The solubility of silica can be changed by controlling the pH of the solution. High solubility in the particulate gel solution results in a strong network.

After aging, the gel is dried. Mainly due to capillary forces, the gel network shrinks during drying. The amount of shrinkage depends on the strength of the network. In the case of a weak polymer network, the volume may be reduced even by a factor of ten compared with the original gel.

The materials used in this study are particulate silica gels whose typical specific surface area, pore volume, and mean pore diameter are  $100 - 800 \text{ m}^2/\text{g}$ ,  $0.4 - 1.2 \text{ cm}^3/\text{g}$ , and  $10 - 200 \text{ \AA}$ , respectively. The pores are voids between the particles, and therefore it is clear that they are not exactly ideally cylindrical in shape, regardless of the smoothing of the geometry caused by coarsening. Pore size and volume depend on particle size and the packing geometry.

### **3.3 Methods for characterization of porous materials**

#### ***3.3.1 Mercury porosimetry***

Surface tensions between the gas, liquid, and solid phases determine whether a liquid can flow inside a pore. If the liquid is non-wetting, it will not penetrate inside the pore without external pressure. Mercury is an example of a non-wetting liquid. When a porous

material is immersed in mercury, the pressure  $P$  required for the penetration of the liquid inside the pore is inversely proportional to the pore radius  $R_p$  [24]:

$$P = \frac{-2\sigma(P,T)\cos\theta}{R_p}. \quad (3)$$

This is the so-called Washburn equation. Here,  $\sigma(P,T)$  is the surface tension of mercury and  $\theta$  is the contact angle, i.e. the angle between the tangents of the surface of the solid and the surface of the liquid measured inside the liquid.

In the mercury porosimetry method [24,25], the total volume of mercury that penetrates into the pores is measured as a function of pressure. At the smallest pressures, mercury can penetrate only into the largest pores, and the higher the pressure is, the smaller are the pores which are filled. The total volume of penetrated mercury determines the volume of the pores with a radius larger than the radius corresponding to the pressure calculated with Eq. (3). Hence, the pore size distribution of the material can be obtained by differentiating the volume vs. radius curve with respect to  $R_p$ .

The range of applications of mercury porosimetry is very wide, as it can be used to determine pore sizes from 3 nm to 400  $\mu\text{m}$  in diameter. However, there are some disadvantages. The high pressures used in the method may damage the porous material. In addition, inkbottle shaped pores, i.e. pores with a narrow neck at the entrance, may cause distortion in the observed pore size distributions, because high pressure is needed to overcome the resistance caused by the neck. ISO standardization of mercury porosimetry for pore characterization is under development [26].

### 3.3.2 Gas Adsorption

Accumulation of gas on the surface of solid is called adsorption. The type of interaction of the molecule with the surface divides the concept into two subgroups, physisorption and chemisorption. In the former, the molecule adheres to the surface without forming chemical bonds, usually by van der Waals forces or electrostatic attraction, whereas the formation of chemical bonds leads to the latter. A solid substance that attracts gas molecules to its surface is called adsorbent, and the term adsorbate refers to the adsorbed molecules.

The adsorption isotherm is the relation between the quantity adsorbed and the partial pressure of the gas phase under equilibrium condition at constant temperature. The shape of the adsorption isotherm depends on the properties of the solid. Therefore, if enough theoretical and experimental knowledge about adsorption is available, the adsorption isotherm can provide useful information about the solid. The adsorption phenomena are especially pronounced when the solid is porous, because then the total surface area is very large.

One commonly used theory for analysis of the adsorption isotherm was developed by Brunauer, Emmett, and Teller (the so-called BET isotherm) [24,25,27]. The BET theory concerns the exchange between the gas phase and the adsorbed layer. The surface of the solid adsorbent is considered to consist of a set of adsorption sites, and each site can adsorb one molecule. A gas molecule may condense onto the surface, stay there a certain

time  $\tau$ , and then evaporate again. Similar condensation may take place in the subsequent molecular layers, and dynamic equilibrium must prevail in each layer. This treatment leads to the BET equation [25]

$$\frac{n}{n_1} = \frac{C P/P_s}{(1 - P/P_s)(1 + (C-1)P/P_s)}, \quad (4)$$

which represents the relationship between the amount of adsorbed gas,  $n$ , and the equilibrium pressure,  $P$ . Here,  $n_1$  is the amount of gas needed to cover the whole surface of the adsorbent with a monolayer,  $C$  is the BET parameter, and  $P_s$  is the saturation pressure of the gas. Parameter  $n_1$  can be solved by fitting the BET equation to the adsorption isotherm, and if the cross-sectional surface area of the gas molecule is known, the total (specific) surface area of the material can be calculated.

There is a hysteresis loop in adsorption isotherms measured from mesoporous materials that the BET equation can not explain. The hysteresis is a consequence of differences in the condensation and evaporation processes in the adsorption and desorption branches. In a cylindrical pore, filling of the pore takes place by means of layer-by-layer adsorption throughout the pore, but evaporation from the full pore takes place from the meniscus of the liquid at the end of the pore. The liquid begins to evaporate when the equilibrium pressure of the system is lowered to the critical pressure  $P$  determined by Kelvin's equation [25]

$$\ln \frac{P}{P_s} = - \frac{2\sigma V_{\text{ads}}}{R_p RT} \cos \theta. \quad (5)$$

Here,  $\sigma$  and  $V_{\text{ads}}$  are the surface tension and the molal volume of the liquid adsorbate,  $R$  is the universal gas constant,  $T$  is the temperature, and  $\theta$  is the contact angle.

Using the Kelvin equation and the desorption branch of the adsorption isotherm, the total volume  $V$  of the pores smaller than the  $R_p$  corresponding to the pressure  $P$  can be calculated. Furthermore, the pore size distribution can be determined by differentiating the  $V$  vs.  $R_p$  curve with respect to  $R_p$ . However, this treatment includes many serious approximations related to the geometry of the pores, the contact angle, and the density and surface tension of the adsorbate. These may cause significant error in the determined distributions.

Gas adsorption is best suited for analyzing the properties of mesoporous materials, although it has also been used for the characterization of micro- and macroporous materials. ISO standardization of the method is in progress [28].

### 3.3.3 NMR relaxometry

Investigation of the properties of porous materials using NMR relaxometry is based on the fact that the interactions between the fluid molecules confined to the pores and the pore walls change the NMR relaxation times [29,30]. It has been proven that the longitudinal ( $T_1$ ) and transverse ( $T_2$ ) relaxation times of the fluid molecules are inversely proportional to the volume-to-surface area ratio,  $V_p/S_p$ , according to the following equation [30]:

$$T_{1,2} = \frac{1}{\rho_{1,2}} \frac{V_p}{S_p} \alpha \frac{1}{\rho_{1,2}} R_p. \quad (6)$$

Here,  $\rho_{1,2}$  is the surface relaxivity for longitudinal and transverse relaxation. In addition, it has been assumed that the  $V_p/S_p$  ratio is directly proportional to the pore radius  $R_p$ . The distribution of the relaxation times observed from the porous sample reflects the pore size distribution.

The prerequisite for using Eq. (6) is that the pore is so small that the fluid molecules collide many times with the pore wall during their contribution to the NMR signal, and this imposes the upper size limit of the method. Surface relaxivity is material dependent, and it must be determined separately for each material before pore sizes can be determined.

### 3.3.4 NMR cryoporometry

The melting point of a substance confined to a small pore is lower than that of a bulk substance. According to the Gibbs-Thompson equation [31], the melting point depression  $\Delta T_{mp}$  is inversely proportional to the pore radius  $R_p$ :

$$\Delta T_{mp} = T_{mp}(\text{bulk}) - T_{mp}(\text{pore}) = \frac{2\sigma_{sl} T_{mp}(\text{bulk})}{\Delta H_f \rho_s R_p} \equiv \frac{k_p}{R_p}. \quad (7)$$

Here  $T_{mp}(\text{bulk})$  and  $T_{mp}(\text{pore})$  are the melting points of the bulk and confined substances, respectively,  $\sigma_{sl}$  is the surface energy of the solid-liquid interface,  $\Delta H_f$  is the specific bulk enthalpy of fusion, and  $\rho_s$  is the density of the solid. The constant  $k_p$  is characteristic of each probe substance.

In NMR cryoporometry [32], melting of a confined substance as a function of temperature is monitored by  $^1\text{H}$  NMR spectroscopy. Because usually the relaxation time in a solid is much shorter than that in a liquid, it is possible to exclusively measure the signal of the unfrozen liquid component by adding a small delay after the excitation pulse or by using a spin-echo pulse sequence. Hence, the intensity of the signal is directly proportional to the total volume of the pores with a radius smaller than the  $R_p$  corresponding to the measurement temperature  $T$  in Eq. (7), and the pore size distribution can be resolved by differentiating the volume vs. radius curve by  $R_p$ .

NMR cryoporometry can be used mainly to determine the pore size of mesoporous materials. In the case of larger pores, the melting point depression is very small, and the temperature resolution sets a limit for reliable pore size determination. In very small pores, the confined substance does not freeze at all. The oversimplified theory on melting in the pores, the unfrozen liquid layer in the surface of the pore, and the gradual melting of the small crystals may cause distortions in the pore size distributions obtained using NMR cryoporometry.

## 4 Xenon porometry

The novel xenon porometry method developed during this study for the characterization of porous materials is based on two ideas: First, instead of observing the NMR active nuclei of the framework of the material, xenon atoms are used as probe atoms because the chemical shift of the  $^{129}\text{Xe}$  isotope is known to be extremely sensitive to its local environment. Secondly, the diffusion of xenon is slowed down by using a medium, which is a solid or a liquid, so that the NMR signal of a xenon atom would more exactly represent the properties of a single pore, and the composite signal of all the atoms in the sample would represent the distribution of the properties. In this chapter, the basics of the method are summarized.

### 4.1 Sample

The sample used in the xenon porometry experiment consists of three components: a solid porous material, an organic substance which acts as a medium, and xenon gas. The typical sample tube construction used in this study is shown in Figure 2.

Each sample component should fulfill certain requirements. The porous material must contain open pores so that the medium and xenon gas can enter the pores. The medium must be in a liquid state when the components of the sample are mixed. In addition, the medium should be a wetting liquid so that it fills all the pores. The melting point temperature, the density change in the liquid-solid phase transition, and the solubility of xenon are the other important properties of the medium that determine, for example, the range of pore sizes where the method is applicable. It is recommended that xenon gas is  $^{129}\text{Xe}$  isotope-enriched in order to achieve a good signal-to-noise ratio. In the case of a liquid medium, it is also possible to use hyperpolarized xenon. The xenon pressure in the sample must be the same as in the calibration measurements of the method.

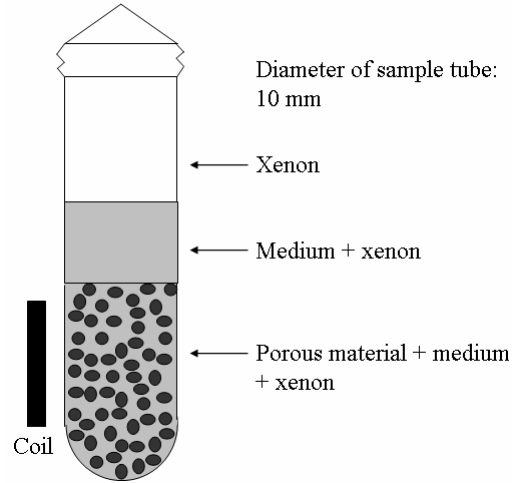


**Figure 2. Typical sample construction used in this study. The amount of added xenon gas corresponds to a pressure of 3.5 atm in an empty sample tube.**

## 4.2 Spectra

The spectra observed from the sample can be divided into three classes according to the phase of the medium (see Figure 3).

Above the melting point of the bulk medium,  $T_{mp}(\text{bulk})$ , all of the media in the sample are in the liquid phase. Two signals are observed, one from xenon dissolved in the bulk medium in between the particles of the porous material (denoted by B) and the other from xenon in the confined medium inside the pores (denoted by C).

Below  $T_{mp}(\text{bulk})$ , the bulk medium freezes. In the case of many substances, the liquid-solid phase transition is accompanied by a significant increase in the density and an abrupt decrease in the solubility of xenon. If this kind of a substance is used as the medium, empty voids (pockets) build up in between the particles of the porous material due to contraction of the medium during freezing. Xenon atoms squeeze out from the solidified medium, and a part of them ends up in the pockets, producing a new signal (denoted by G) in the spectrum. Because the pockets are relatively large, the chemical shift of signal G is close to that of bulk xenon gas. On the basis of the Gibbs-Thompson equation, Eq. 7, the melting point of the confined liquid,  $T_{mp}(\text{pore})$ , is lower than that of bulk liquid, and signal C is still seen at the temperatures between  $T_{mp}(\text{pore})$  and  $T_{mp}(\text{bulk})$ . The intensity of signal C increases in the liquid-solid phase transition, because part of the xenon released from the solidified bulk medium ends up in the confined liquid.

When the temperature is lowered below  $T_{mp}(\text{pore})$ , the confined medium solidifies and pockets also build up inside the pores because of the contraction of the medium. However, these pockets are much smaller than those in between the particles of the porous material. Again, xenon atoms squeeze out from the solidified medium and a part of them ends up in the pockets and produces a new signal, signal D. The chemical shift of

signal D is larger than that of signal G because of the smaller size of the pockets inside the pores. A residual signal C is still usually observed at those temperatures. It arises from small unfrozen pores and from an unfrozen liquid layer on the surface of the pores. Evidently, a part of the xenon atoms released from the solidified confined medium ends up in the unfrozen liquid, increasing the intensity of signal C.

If the melting point of the medium is low, measurement of the signals from all the classes represented in Figure 3 may require very low temperatures, in which case the liquefaction of xenon may cause changes in the spectrum. The signal of liquefied xenon may appear in the spectra at very high chemical shifts ( $\sim 240$  ppm). In addition, the chemical shift of signal D may increase rapidly with decreasing temperature due to the liquefaction of xenon inside the pockets. The effects of the liquefaction have been analyzed in detail in Paper I.

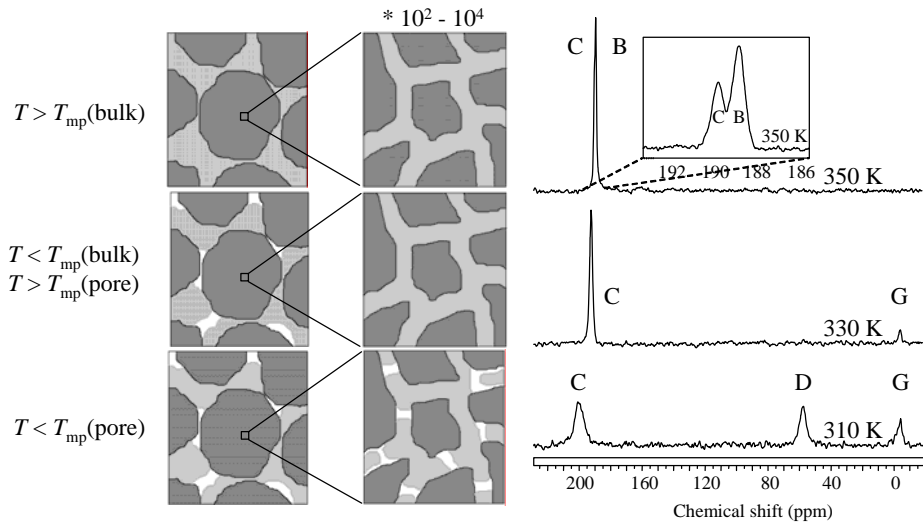


**Figure 3.** The medium between the particles of the porous material (left) and inside the pores (middle) at different temperatures (far left), and the spectra observed from the sample (right). In the pictures, dark gray represents the porous solid, light gray the medium and white the pockets.

### 4.3 Pore size determination using a solid medium

As explained above, signal D arises from xenon inside the pockets built up in the pores due to contraction of the medium in the liquid-solid transition. If it is assumed that the length to radius ratio of the medium in a cylindrical pore does not change during contraction, it can be deduced that the pocket volume is composed of an empty pore segment and a thin layer between the pore wall and the solidified medium, as is illustrated in Figure 4 (c). Furthermore, if a fast exchange of xenon atoms takes place between the adsorbed site on the walls of the pocket and in the free volume site in the middle of the pocket, the chemical shift of xenon depends on the surface-to-volume ratio

of the pocket. On the basis of the geometry of the pocket, it can be shown that the surface-to-volume ratio is proportional to pore size, and therefore the following relationship exists between the chemical shift,  $\delta$ , and the pore radius,  $R_p$  (see details in Paper III):

$$\delta = \frac{\delta_s}{1 + \frac{bR_p}{a}}. \quad (8)$$

Here,  $\delta_s$  is the chemical shift of a xenon atom adsorbed on the surface of the pocket,  $a = KRT$ , where  $K$  is Henry's constant and  $R$  is the universal gas constant. Parameter  $b$  depends on the geometry of the pocket.

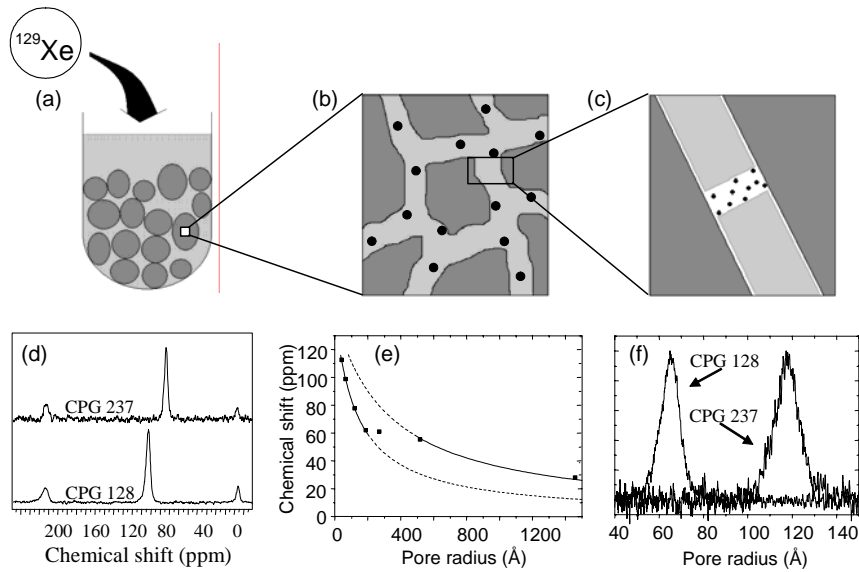


**Figure 4. Determination of pore size distribution by xenon porometry using a solid medium. The porous material is immersed in a liquid medium, and xenon gas is added to the sample (a). Dissolved xenon atoms (dots) diffuse inside the pores (b). During freezing, empty pockets build up in the pores due to contraction of the medium and xenon squeezes out from the solidifying medium into the pockets (c). The chemical shift of xenon inside the pocket depends on the pore size, and the distribution of the signals observed from the different pores represents the pore size distribution (d). Using the determined correlation (e), the pore size distribution can be obtained by converting the chemical shifts to pore radii (f).**

The critical pore radius  $R_c$  divides the behavior of the chemical shift of signal D as a function of pore size into two regions. In pores smaller than  $R_c$ , the layer between the pore wall and the solidified medium is so small that a xenon atom does not fit inside, and all the atoms contributing to signal D are inside the empty pore segment, as is illustrated in Figure 4 (c). However, when the size of the pore exceeds the critical pore size, xenon atoms can enter inside the layer, and this substantially increases the total surface-to-volume ratio of the pocket. In the model (8), this leads to a reduction of the  $b$  value and



consequently to higher chemical shifts than could be extrapolated from the trend in smaller pore sizes.

Because there is a one-to-one correspondence between pore size and the chemical shift of xenon inside the pocket, and because a solid medium prevents the xenon atoms from diffusing between the different pores, the chemical shift of a xenon atom is characteristic of the size of one pore. The atoms in pores of different sizes produce separate signals with characteristic chemical shifts, and the composite signal from all the pores in the sample (signal D) represents the pore size distribution. If the line width of the resonance signal of one pocket is small, the pore size distribution can be determined simply by converting the chemical shift scale of signal D into the pore radius scale using the correlation (8), where the parameters are experimentally determined by means of calibration samples (see Figure 4).

In the case of the materials used in this work, a comparison of the pore size distributions obtained using this simple conversion method with those measured by manufacturers shows that neglecting the intrinsic line width is a very good approximation when the pore size is smaller than  $R_c$ . In the case of larger pores, however, the relatively slow exchange of xenon between the empty pore segment and the layer between the pore wall and the solid medium makes the intrinsic line width larger, and then determination of the pore size distribution is a much more complicated process. The pore shape distribution and the pore orientation-dependent magnetic susceptibility might have their own contributions to the chemical shift and the shape of signal D, although they have been proven to be of minor importance in these studies.

The melting point and the density behavior in the liquid-solid transition are the most important properties of the medium, when pore sizes are determined by means of signal D. If the melting point is sufficiently high, the measurements can be done near room temperature, and no cooling setup is needed. The range of applications of the method can be varied by using media with different density changes at the freezing transition. If the density change is small, the critical pore radius is large, which makes it possible to determine the pore size distribution of large pores. On the other hand, if the change is large, the pockets are large, and they are also formed in very small pores. The use of this kind of medium makes the method most sensitive to small pore sizes.

Because the walls of the pockets are mainly composed of the solid medium, xenon atoms interact largely with the medium, and not so much directly with the walls of the pores. This makes the method more universal for the characterization of pore geometry as compared with the experiments, where pure xenon gas is absorbed inside the pores, because then the observed signal is also more characteristic of the surface material of the pore.

#### **4.4 Pore size determination using a liquid medium**

Signals B and C arise from xenon dissolved in bulk and confined liquid, respectively. The chemical shift of signal C is larger than that of signal B due to the interactions of xenon atoms with the pore wall. These interactions may take place either directly or through the liquid medium. As a consequence of the interactions, the chemical shift of signal C is

dependent on pore size (see Figure 5 (b)), and this dependence can be utilized in pore size determination.

Unfortunately, the chemical shift of signal C is also very sensitive to temperature, and a small temperature difference between the actual measurement and the calibration measurements of the correlation between the chemical shift and pore size may cause a significant error. However, because the temperature dependence of the chemical shift of signal B is very similar to that of signal C, the error caused by the inaccuracy of the temperature can be eliminated by comparing the difference in the chemical shifts of signals C and B instead of the chemical shift of signal C with respect to the gas reference signal (see Figure 5 (c)).

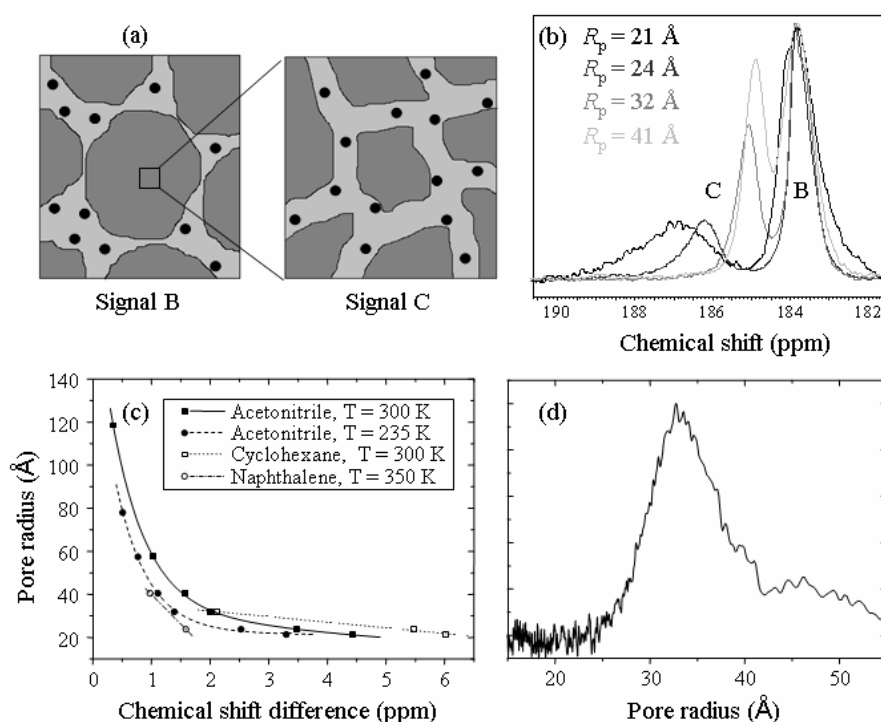


**Figure 5. Pore size determination by xenon porometry using a liquid medium. Signal B arises from xenon dissolved in bulk liquid between particles of porous material, and signal C from that in the confined liquid inside the pores (a). The difference in the chemical shifts of signals C and B is dependent on pore size (b). If the correlation is known (c), the mean pore size or even the pore size distribution of the material can be determined (d).**

If the correlation between the pore radius and the differences in the chemical shifts of signals C and B has been determined by using calibration samples, the mean pore radius of the porous material can be calculated by means of the difference. The shape of the signal represents the pore size distribution if the diffusion is slow enough. This is not evident on the basis of the root-mean-square distances traveled by dissolved xenon during the time scale of the NMR experiment estimated by means of the translational diffusion

coefficients of the bulk liquid. However, the EXSY spectra presented in Paper IV imply that in certain cases diffusion in confinement is really so slow that the shape of signal C represents the pore size distribution satisfactorily.

As in the case of signal D, the intrinsic line width, pore geometry distribution, and pore orientation-dependent magnetic susceptibility may also affect the chemical shift and shape of signal C besides the pore size distribution, and their significance should be known in the analysis in order to avoid misinterpretation. However, they seem to be of minor importance in the current studies.

As it can be deduced from Figure 5 (c), the range of applications of signal C in pore size determination is quite restricted compared with that of signal D. In the case of the media used in this study (acetonitrile, cyclohexane and naphthalene), it is possible to measure pore radii smaller than  $\sim 60 \text{ \AA}$  by means of the chemical difference between signals C and B. When the radius is larger, the signals merge together. On the other hand, there are some advantages in the use of signal C instead of signal D for pore size determination. First, media that are in a liquid state at room temperature are easy to handle in the sample preparation, and signal C is observed at room temperature from samples containing this kind of medium. Secondly, a liquid medium makes it possible to use hyperpolarized xenon to enhance the signal-to-noise ratio, whereas a solid medium prevents the hyperpolarized xenon from penetrating inside the pores. Third, it is possible to trace the flow of the solution through the porous sample by conventional or remote detection techniques [33-35]. In this case, the time resolution of the experiment is much better than when the flow of pure gas is detected, because the medium slows down the diffusion, but there is still chemical shift information about pore sizes in the spectra or images. In addition, the long relaxation time of dissolved xenon (on the order of 100 s) makes it very usable for remote detection experiments.

#### 4.5 Pore size determination by melting point depression

The spectra measured from the xenon porometry sample as a function of temperature (see Figure 3) contain much information about the phase transition temperatures of the medium: The melting point of the bulk medium can be observed from the appearance of signal B, the disappearance of signal G, and changes in the intensity of signal C, whereas the disappearance of signal D and an increase in the intensity of signal C reveal the melting point of the confined liquid. On the other hand, according to the Gibbs-Thompson equation, Eq. (7), the melting point of a substance confined to a pore is inversely proportional to pore size. Therefore, it is possible to estimate the average pore size of the material on the basis of the melting point depression deduced from the spectra. However, the minor effects of dissolved xenon on the melting temperatures studied in paper II must be taken into account.

Contrary to the NMR cryoporometry experiment, it is not possible to observe the relative volume of the liquid phase as a function of temperature in the xenon porometry experiment, because the concentration of xenon in the liquid phase changes at the phase transition points as a part of the xenon atoms moves from the solidifying phase to the

liquid phase. Therefore, the detailed pore size distribution cannot be determined by means of the phase transition information in the spectra.

If there are no fixed time restrictions, it is advantageous to measure the spectra from the xenon porometry sample over a wide temperature range, because then the information of all three methods discussed above is available. In this case, the pore sizes obtained by means of phase transition points can be used for the confirmation of the other results. Furthermore, if the geometry of the porous structure in the sample is very complicated, the complementary information provided by the three methods may be a key to understanding the structure, because the methods relate differently to the geometry.

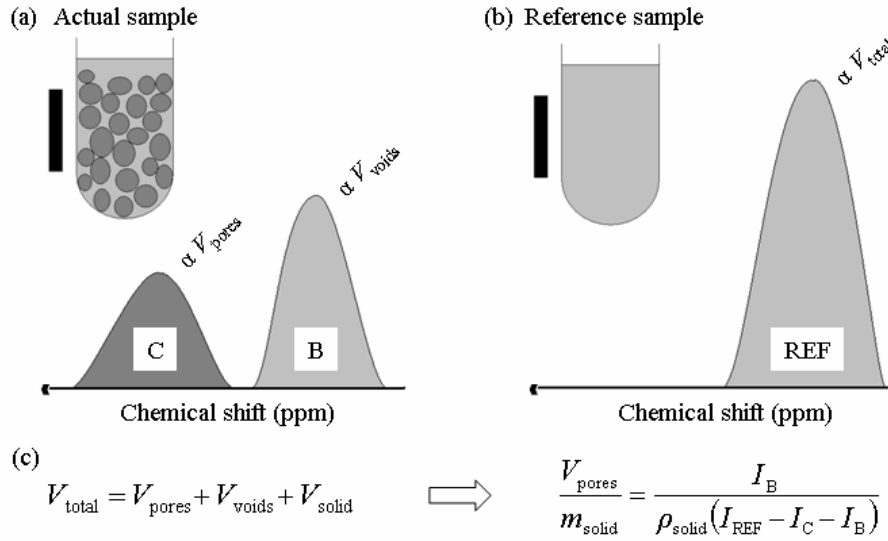


**Figure 6. Determination of porosity by xenon porometry.** The integrated intensities of signals C and B from xenon dissolved in confined and bulk liquid are directly proportional to the volumes of the pores ( $V_{\text{pores}}$ ) and the voids between the particles of porous material ( $V_{\text{voids}}$ ), respectively, and if the solubility of xenon in the phases is the same, the proportionality constant is also the same (a). The intensity of the signal from a reference sample containing only liquid and xenon is proportional to the total volume ( $V_{\text{total}}$ ) of the sample in the measurement region (b). Because the total volume is a sum of the volumes of the pores, voids, and solid skeleton ( $V_{\text{solid}}$ ), the porosity (the volume of the pores divided by the mass of the solid,  $V_{\text{solid}}/m_{\text{solid}}$ ) of the sample can be calculated if the density of the solid skeleton ( $\rho_{\text{solid}}$ ) is known (c).

#### 4.6 Porosity determination

The total volume of a sample containing porous material is a sum of the volumes of the pores, the solid skeleton of the material, and the voids between the particles. In the xenon porometry experiment, the intensities of the signals of xenon dissolved in bulk and confined liquid are proportional to the volumes of the voids and pores, respectively, if the

liquid fills all the empty spaces. The proportionality constant is the same if the solubility of xenon is the same in both phases. In this case, the ratio of the intensities of signals C and B corresponds exactly to the ratio of the volumes of the pores and voids. Hence, the porosity (the volume of the pores divided by the mass of the solid) of the material can be resolved if the intensities can be scaled in the real dimensions. This can be done if the density of the solid skeleton and the mass of the material are known. Another possibility for scaling is to measure the intensity of the signal of the dissolved xenon from a sample of the same size that contains only liquid and xenon (see Figure 6). In this case, the xenon concentration in the liquid must be the same as in the actual sample, and the density of the solid skeleton is also needed.

The experiments carried out in this study show that the assumption that xenon solubility in the bulk and confined phase is the same is a very good approximation, because the measured porosities are in good agreement with those announced by the manufacturers. However, the fact that the intensity ratio of signals B and C depends slightly on temperature reveals that solubility is not exactly the same in the phases, and this should be taken into account in very precise measurements.

The prerequisite for porosity measurements is that signals B and C are far enough from each other so that their intensities can be determined reliably. In the case of the media used in this study, this is true when the pore radius is less than  $\sim 60 \text{ \AA}$ .

## 5 Conclusions

The present thesis shows that  $^{129}\text{Xe}$  NMR of xenon dissolved in a medium confined in a porous material is very sensitive to the geometry of the porous network. Because the medium slows down the diffusion of xenon, the signal of a particular xenon atom is characteristic of the very local properties of the material, and the signals of all the xenon atoms in the different parts of the sample represent the distribution of certain properties of the sample.

In this work, special attention was placed on investigating how pore size is reflected in the spectra observed at different temperatures above and below the melting points of the medium. Three different ways of determining pore sizes have been proposed: two on the basis of the chemical shifts of the signals, and one by means of the phase transition temperatures revealed by the spectra. It has been shown that in certain cases the correlation between the chemical shift and pore size makes it possible to determine the pore size distribution in a very simple way by converting the chemical shift scale of the spectrum into a pore radius scale.

Apart from pore sizes, there are other things that may affect the above correlations, such as the shape distribution of the pores and pore orientation-dependent magnetic susceptibility. In such a case, the use of all the above-mentioned methods can give valuable complementary information about the sample, because they experience these effects differently.

It has also been proved that the porosity of the sample can be determined by means of the intensities of two signals observed from the liquid medium.

The range of applications of xenon porometry depends on the correlation used. The mean pore radius of the material can be measured up to the micrometer range by means of the chemical shift of signal D arising from the pockets built up during the freezing of the medium. However, determination of the pore size distribution may be limited by the critical pore radius if the effect of the exchange of xenon between the empty pore segment and the layer between the pore surface and the solidified medium on the line width is not known. In the case of the solid media used in this study (acetonitrile and naphthalene), the critical pore radius is about 200 Å, but its value can be modified by using media with different density changes in the liquid-solid phase transition.

The difference in the chemical shifts of signals B and C originating from xenon dissolved in bulk and confined liquid is less sensitive to pore size than the chemical shift of signal D. In the case of the liquid media used in this study (acetonitrile, naphthalene and cyclohexane), the signals merge together when the pore radius is larger than about 60 Å, and this determines the upper limit of the pore size measurements. Actually, this is also the limit for porosity determination, because it is made by means of the intensities of the same signals, and accurate determination of the intensities requires well resolved signals.

The temperature resolution and the value of constant  $k_p$  in the Gibbs-Thompson equation (Eq. 7) set the upper limit of pore size determination by means of the melting point depression observed from the changes in the spectra. In principle, the temperature resolution of a spectrometer may be tenths of a degree, but in practice the temperature gradient in the sample area and the broadening of the phase transition temperature regions caused by impurities in the sample decreases the resolution to at least one degree. The value of  $k_p$  typically varies between 500 and 1000 KÅ, depending on the medium, and therefore the upper limit of pore size determination with this temperature resolution is about 500 – 1000 Å.

The lower limits of the measurements depend on whether the medium freezes in the very small pores at all and whether the dissolved xenon can enter the small pores, among other things. It is evident that the pore sizes and the porosities of the materials can be determined down to the microporous range by means of xenon porometry.

The above discussion shows that the range of applications of xenon porometry is very wide compared with that of all the other methods described in section 3.3 except for mercury porosimetry.

Degassing, adding the xenon gas and sealing the sample tube make sample preparation in xenon porometry quite time-consuming and tedious. On the other hand, when analyzing large amounts of samples the preparation process can be done automatically. Xenon porometry measurements can be done very easily and quickly. Measurement of one spectrum takes from a couple of seconds to ten minutes, depending on how much accumulation is needed in order to obtain a sufficient signal-to-noise ratio. If temperature stabilization is needed, it increases the measurement time by about twenty minutes. The measurement does not destroy the material. Interpretation of the spectra is easy on the basis of the information presented in this thesis, and the pore size distribution can be resolved using simple mathematical conversions. The entire analysis can be automated.

In summary, xenon porometry is a quick, simple and versatile method for characterizing porous materials, and it does not destroy the material. It is a scientifically fascinating method and it has a large potential for applications in industry.

## References

- 
- [1] Dullien FAL (1992) Porous media: Fluid Transport and Pore Structure. Academic Press, San Diego; 2<sup>nd</sup> edition.
- [2] Abragam A (1961) The Principles of Nuclear Magnetism. Oxford University Press, Oxford.
- [3] Ernst RR, Bodenhausen G & Wokaun A (1987) Principles of Nuclear Magnetic Resonance in One and Two Dimensions. Oxford University Press, Oxford.
- [4] Levitt MH (2001) Spin Dynamics: Basics of Nuclear Magnetic Resonance. John Wiley & Sons, Chichester.
- [5] Ratcliffe CI (1998) Annu Rep NMR Spectrosc 36: 123.
- [6] Raftery D & Chmelka BF (1994) NMR Basic Principles and Progress 30: 111.
- [7] Jokisaari J (1994) Prog NMR Spectrosc 26: 1.
- [8] Walker TG & Happer W (1997) Reviews of Modern Physics 69: 629.
- [9] Goodson BM (2002) J Magn Reson 155: 157.
- [10] Fraissard J & Ito T (1988) Zeolites 8: 350, and references therein.
- [11] Springuel-Huet MA, Bonardet JL & Fraissard J (1995) Appl Magn Reson 8: 427.
- [12] Demarquay J & Fraissard J (1987) Chem Phys Lett 136: 314.
- [13] Ripmeester JA, Ratcliffe CI & Tse JS (1988) J Chem Soc Faraday Trans 84: 3731.
- [14] Chen F, Chen CL, Ding S, Yue Y, Ye C & Deng F (2004) Chem Phys Lett 383: 309.
- [15] Tserkikh VV, Moudrakovski IL & Mastikhin VM (1993) J Chem Soc Faraday Trans 89: 4239.
- [16] Tserkikh VV, Moudrakovski IL, Breeze SR, Lang S, Ratcliffe CI, Ripmeester JA & Sayari A (2002) Langmuir 18: 5653.
- [17] Kärger J & Ruthven DM (1992) Diffusion in Zeolites and Other Microporous Solids. John Wiley & Sons, USA.
- [18] Jeener J, Meier BH, Bachmann P & Ernst RR (1979) J Chem Phys 71: 4546.
- [19] Morey GW (1954) The Properties of Glass. Reinhold, New York; 2<sup>nd</sup> edition.
- [20] Haller W (1965) Nature 206: 693.
- [21] Haller W (1983) Chemical Analysis 66: 535.
- [22] Brinker CJ & Scherer GW (1989) Sol-Gel Science. Academic Press, San Diego.
- [23] Iler RK (1979) The Chemistry of Silica, Wiley, New York.
- [24] Keller JU & Staudt R (2005) Gas Adsorption Equilibria: Experimental Methods and Adsorption Isotherms. Springer, New York.
- [25] Gregg SJ & Sing KSW (1982) Adsorption, Surface Area, and Porosity. Academic Press, New York; 2<sup>nd</sup> edition.
- [26] International Standardisation Organization, Geneva (ISO), ISO/FDIS 15901-1: Evaluation of Pore Size Distribution and Porosimetry of Solid Materials by Mercury Porosimetry and Gas Adsorption -- Part 1: Mercury Porosimetry.
- [27] Brunauer S, Emmett PH & Teller E (1938) J Am Chem Soc 60: 309.



- 
- [28] International Standardisation Organization, Geneva (ISO), ISO/DIS 15901-2 and 15901-3: Pore Size Distribution and Porosimetry of Solid Materials by Mercury Porosimetry and Gas Adsorption -- Part 2: Analysis of Mesopores and Macropores by Gas Adsorption. -- Part 3: Analysis of Micropores by Gas Adsorption.
- [29] Kimmich R (1997) NMR: Tomography, Diffusometry, Relaxometry. Springer, New York.
- [30] Stallmach F & Kärger J (1999) Adsorption 5: 117.
- [31] Jackson CL & McKenna GB (1990) J Chem Phys 93: 9002.
- [32] Strange JH & Rahman M (1993) Phys Rev Lett 71: 3589.
- [33] Moulé AJ, Spence MM, Han S, Seeley JA, Pierce KL, Saxena S & Pines A (2003) Proc Natl Acad Sci USA 100: 9122.
- [34] Seeley JA, Han S & Pines A (2004) J Magn Reson 167: 282.
- [35] Granwehr J, Harel E, Han S, Garcia S & Pines A (2005) Phys Rev Lett 95: 075503 1.

## Original papers

- I Reproduced with permission from the Journal of Physical Chemistry B, Telkki V-V, Lounila J & Jokisaari J. Behavior of Acetonitrile Confined to Mesoporous Silica Gels As Studied by  $^{129}\text{Xe}$  NMR: A Novel Method for Determining the Pore Sizes. 109: 757-763. Copyright (2005), **American chemical society**.
- II Reproduced with permission from the Journal of Physical Chemistry B, Telkki V-V, Lounila J & Jokisaari J. Determination of Pore Sizes and Volumes of Porous Materials by  $^{129}\text{Xe}$  NMR of Xenon Gas Dissolved in a Medium. 109: 24343-24351. Copyright (2005), **American chemical society**.
- III Reproduced with permission from the Journal of Chemical Physics, Telkki V-V, Lounila J & Jokisaari J. Xenon Porometry at Room Temperature. In press. Copyright (2006), **American Institute of Physics**.
- IV Reproduced with permission from the Physical Chemistry Chemical Physics, Telkki V-V, Lounila J & Jokisaari J. Influence of Diffusion on Pore Size Distributions Determined by Xenon Porometry. Submitted. Copyright (2006), **Royal Society of Chemistry**.